Everest Advances in Science and Technology (EAST) Vol. 2, No. 1, 2026 (Special Issue)
ISSN: 3102-0410 (Print), 3102-0429 (Online)
DOI: https://doi.org/10.3126/east.v2i2.99474

Mechanical Performance Evaluation of M20 Concrete with Rice Husk Derivatives

RISHIKESH YADAV[1], SHREEYASH ACHARYA[1], SANGINA LAMICHHANE[1], GOKARNA BAHADUR MOTRA[2,3,*], KHEM RAJ SHRESTHA[2,*]

Abstract. In the context of Nepal, rice production generates considerable amounts of agricultural waste, notably rice husk. This study inspects the performance of M20 grade concrete incorporating rice husk and its derivatives, such as rice husk ash (RHA) and rice husk biochar (RHB), as partial replacement of cement by weight. A replacement level of 5% for each material was selected to evaluate its effect on the workability and mechanical properties. The slump test analysis revealed a minimal decline in workability due to the porous nature and water absorption capacity of the materials. The mechanical strength (compressive) results at 28days exhibited the incremental improvement for mixes containing 5% RHA (28.1MPa) and 5% RHB (26.9 MPa) compared to the control mix (26.4 MPa), while a minimal reduction was noticed for the combined mix, as 15% in total replacement of cement by RH-derivatives (23.7MPa). The development in strength is assigned to the pozzolanic reaction of amorphous silica present in RHA, which assists in the formation of additional calcium silicate hydrate (C-S-H) gel. The presence of chemical bonds such as Si-O-Si bonds, which highlight the silica contribution to the concrete matrix at the time of hydration, can be analyzed by Fourier Transfer Infrared Spectroscopy (FTIR) analysis. The promotion of sustainable construction and efficient agricultural-waste management can be effectively achieved by using rice husk derivatives as supplementary cementitious materials. The study clarifies that the rice husk derivatives can be effectively utilized as supplementary cementitious materials (SCMs), promoting sustainable construction and efficient agricultural-waste management.

Keywords: FTIR, rice husk, rice husk ash, rice husk biochar, sustainable construction concrete

[1] Pulchowk Campus, IOE, Lalitpur, Nepal

[2] Department of Applied Science and Chemical Engineering, IOE, Lalitpur, Nepal

[3] Department of Civil Engineering, IOE, Lalitpur, Nepal

Email: gmotra@ioe.edu.np

* Corresponding author

Manuscript received: 14 March 2026; Revised: 25 June 2026; Accepted: 18 July 2026.

1. INTRODUCTION

1.1. **BACKGROUND.** The most widely used construction material is concrete because of its strength, durability, versatility, and relatively low cost. Concrete is primarily composed of cement, aggregate (coarse and fine), and water, where cement acts as the binding material that provides strength and durability. However, cement production is energy-intensive and contributes significantly to global carbon dioxide (CO_2) emissions, accounting for about 7–8% of total worldwide emissions [1]. Rapid urbanization has magnified environmental concerns due to the increasing demand for cement in the construction industry. The considerable awareness about the environmental impact of the production and use of SCM's derived from agricultural waste promotes the reduction in environmental impact [2].
Rice husk is an abundant agricultural by-product generated during rice milling in enough quantity in Nepal. Rice husk contains high amounts of silica and carbon [3]. Rice husk ash and biochar can be obtained by thermal treatment [4]. The concrete strength can be enhanced by rice husk ash because it possesses the pozzolanic properties and adds additional SCM's to the concrete matrix, whereas biochar possesses the internal curing and water retention due to its porous nature [5]. Voids in the concrete matrix are reduced by rice husk, which acts as a filler.
This study investigates the mechanical performance of M20-grade concrete with rice husk and its derivatives. The slump test is conducted for Fresh concrete properties to evaluate the workability, while hardened concrete specimens are tested to determine compressive strength at different curing ages (7, 14, and 28 days). The chemical and mineralogical properties of incorporated, hardened concrete after 28 days are carried out by advanced material characterization techniques such as Fourier Transform Infrared Spectroscopy (FTIR).

1.2. **PROBLEM STATEMENT.** In modern construction practices, the mechanical performance of concrete has become an important consideration for the sustainability of the structure and the concrete matrix. Researchers have reported the beneficial effects of rice husk ash on the strength and durability of concrete due to its pozzolanic properties and the additional Silica-gel formation in the concrete mix. Similarly, the potential to adjust the pore structure of concrete is due to rice husk, and the hydration characteristics of cement-based materials are governed by biochar and ash. However, most available research has focused on the individual use of rice husk and its derivatives; combined performance in conventional concrete under laboratory conditions has been examined by limited studies [6].
The study investigates the effects of rice husk and its derivatives on the workability, compressive strength, and microstructural characteristics of concrete for different curing ages [7]. The results of this experimental work will contribute to an enhanced understanding of the derivative roles of concrete and provide a basis for their effective utilization in cementitious composites as supplementary cementitious materials.

1.3. **OBJECTIVE.** The main objective is to explore the understanding of the suitability of rice husk and its derivatives as supplementary cementitious materials in M20-grade concrete by evaluating their synergetic and individual effects on the mechanical performance and microstructural characteristics of the concrete mix.
The specific objectives are:

(1) To evaluate the workability of fresh concrete with rice husk and its derivatives using the slump test.
(2) To evaluate the compressive strength of concrete incorporating rice husk-based materials at curing ages of 7, 14, and 28 days.
(3) To compare the mechanical performance of rice husk and its derivatives in M20-grade concrete with that of conventional concrete.
(4) To characterize the incorporated materials' chemical and mineralogical properties of concrete using Fourier Transform Infrared Spectroscopy (FTIR).

1.4. **SIGNIFICANCE OF STUDY.** This study investigates sustainable concrete by exploring the use of rice husk and its derivatives (ash and biochar) as alternative supplementary cementitious

materials in M20-grade concrete. This study addressed the dual challenge of agricultural waste utilization and reduced dependence on conventional cement in the context of the Nepal construction industry.
A key contribution is to the synergetic evaluation of rice husk and its derivatives under identical experimental conditions (laboratory conditions), providing a better understanding of their individual effects on the fresh, mechanical, and microstructural properties of concrete. The results will provide the effective utilization of locally sourced agricultural residues and provide valuable data for the development of sustainable and resource-efficient construction supplementary cementitious materials. The results may also contribute as a baseline for future research on husk-derived cementitious materials and their potential applications in concrete production and the construction industry.

1.5. **LIMITATIONS.** As per the problem of statements and methodology of the study, the present study has the following distinctive limitations:

(1) The evaluation of concrete performance is limited to workability and compressive strength; other mechanical properties, such as tensile strength and flexural strength, are not investigated.
(2) Long-term durability characteristics, including permeability, shrinkage, creep, and resistance to environmental exposure, are beyond the scope of this study.
(3) Material characterization is primarily based on FTIR analyses; advanced microstructural investigations such as Scanning Electron Microscopy (SEM) are not performed.
(4) The experimental work is conducted under controlled laboratory conditions, and the results may differ under real field conditions.
(5) Economic feasibility and large-scale practical implementation of rice husk-derived materials in concrete are not assessed in this study.

2. LITERATURE REVIEW

The most used construction material is concrete, which continues to be a material valued for its strength, durability, adaptability, and cost-effectiveness. However, cement is a key component of concrete, which is energy-intensive and a major source of carbon emissions, promoting interest in sustainable alternatives such as supplementary cementitious materials [1]. The outer layer of rice grains is removed during milling (about 20–22% of the total grain weight). Rice husk is abundant and silica-rich. Improper disposal of husk, such as burning or dumping, causes environmental pollution [8]. Thermal treatment converts rice husk into rice ash and biochar, which are widely studied as supplementary cementitious materials [5]. Its high silica content has made it a subject of growing interest in construction applications. When subjected to thermal processing, husk can be converted into ash and biochar, both of which show promise in enhancing cement-based materials [6, 8].
The raw rice husk consists mainly of cellulose, lignin, and 15–20% silica. Raw rice husk may slightly reduce workability due to the particles' shape and size [8]. Rice husk ash is produced by controlled combustion at 600–800^{0}C, and contains amorphous silica with high pozzolanic activity. It reacts with calcium hydroxide produced during cement hydration to form additional calcium silicate hydrate (C-S-H) gel, thereby enhancing strength and durability [9, 10]. Ash increases compressive strength through pozzolanic reactions, forming C_S-H gel in addition to the mix, with 28-day strength increasing by 2.4–18.7% for 5–20% partial replacement of cement by weight [3].
Rice husk biochar is a carbon-rich, porous substance produced by pyrolysis under limited oxygen, which improves water retention in the concrete for internal curing and influences microstructure and durability [9]. Low-level rice husk biochar, about 1–3% partial replacement of cement by weight, can improve 28-day strength by 10–40%. In the combined use of derivatives as partial replacement, further modifications to concrete strength are used at optimally proportioned dosages [9]. The pozzolanic reaction leads to better strength, lower permeability, and improved long-term durability. The replacement of 10–20% of cement with ash often yields optimal mechanical properties without significantly compromising workability, as suggested by Research [11, 12].

The mechanical performance of modified concrete with ash depends on multiple factors, such as combustion temperature, particle size, replacement level, and curing conditions [13]. Therefore, greater reactivity in concrete mix due to increased surface area by finer ash particles, but their porous nature also raises water demand [14]. Compressive strength, shrinkage resistance, and durability are enhanced with optimal replacement (3–10% by weight of cement); higher amounts increase porosity. Ash affects workability by reducing the slump of fresh concrete due to its fine particles and water absorption, whereas biochar slightly reduces workability at higher levels due to its porosity. Partial replacement of cement with Biochar at a low content of 1–3%, manageable with superplasticizers [15]. When ash is added, slump tends to decrease unless appropriate chemical admixtures are used [16].
Biochar features a porous, carbon-rich structure that absorbs and slowly releases water during hydration, promoting internal curing, produced via pyrolysis under low-oxygen conditions. Biochar has recently gained attention for its potential in concrete production [17]. This process supports more complete hydration, minimizes micro-cracking, and enhances long-term performance [18]. Past studies indicate that low replacement of cement with biochar can improve strength and durability, while higher amounts may increase porosity and weaken the material [19].
In contrast, untreated husk acts mainly as a filler in concrete, particle packing, and support waste reuse; its pozzolanic activity is much lower than that of ash and biochar [20]. Still, some studies have found that limited inclusion of raw husk can enhance matrix density without negatively affecting key engineering properties of concrete [21]. Recent research has explored how the combined use of derivatives improves particle arrangement, how ash contributes to strength through pozzolanic reactions, and how biochar supports internal curing and moisture retention [22]. Well-balanced mixtures of these derivatives have shown improvement in strength, durability, and microstructure compared to conventional concrete [22].
Workability remains a crucial factor in fresh concrete. The high surface area, porosity, and water absorption of ash and biochar tend to reduce slump in high replacement levels [16, 23]. However, the use of suitable chemical admixture can adjust and help to maintain acceptable workability in the mix [24]. Numerous studies confirm that concrete with an optimal ash replacement level exhibits improvement in strength due to enhanced C-S-H formation and a denser pore structure [25]. Similarly, low doses of biochar have been linked to improved hydration and microstructural development, resulting in higher strength [26].
Microstructural analysis techniques like FTIR analysis of rice husk and its derivatives are frequently used to study the hydration products and mineralogical changes in cementitious systems, confirming the additional silica, which contributes to additional C-S-H gel formation in mix and reduced calcium hydroxide in rice husk ash and rice husk biochar mixes [27].

2.1. **Research gaps.** As per the above literature reviews, the gaps in the study of M20 concrete with rice husk derivatives are:

(1) Limited studies on the combined use of rice husk and its derivatives.
(2) Insufficient correlation between fresh properties and hardened performance for a mix of rice husk and its derivatives.
(3) Few studies integrate FTIR on crushed concrete.
(4) Optimization of combined replacement levels is lacking.
(5) Limited quantitative environmental impact assessment.

3. METHODOLOGY

The methodology flowchart represents a systematic experimental process that starts with research planning, moves through material preparation and concrete production, including mixing, placing, casting, curing, testing, and decision-making regarding specimen quality, and ends with data analysis and reporting to evaluate the effectiveness of derivative-based cement matrix in Figure 1. The collection of all required raw materials, such as rice husk, locally sourced from Suryabinayak, Bhaktapur, Nepal, Cement (OPC) from Hongshi Shivam Cement Pvt Ltd., Fine aggregate (sand),

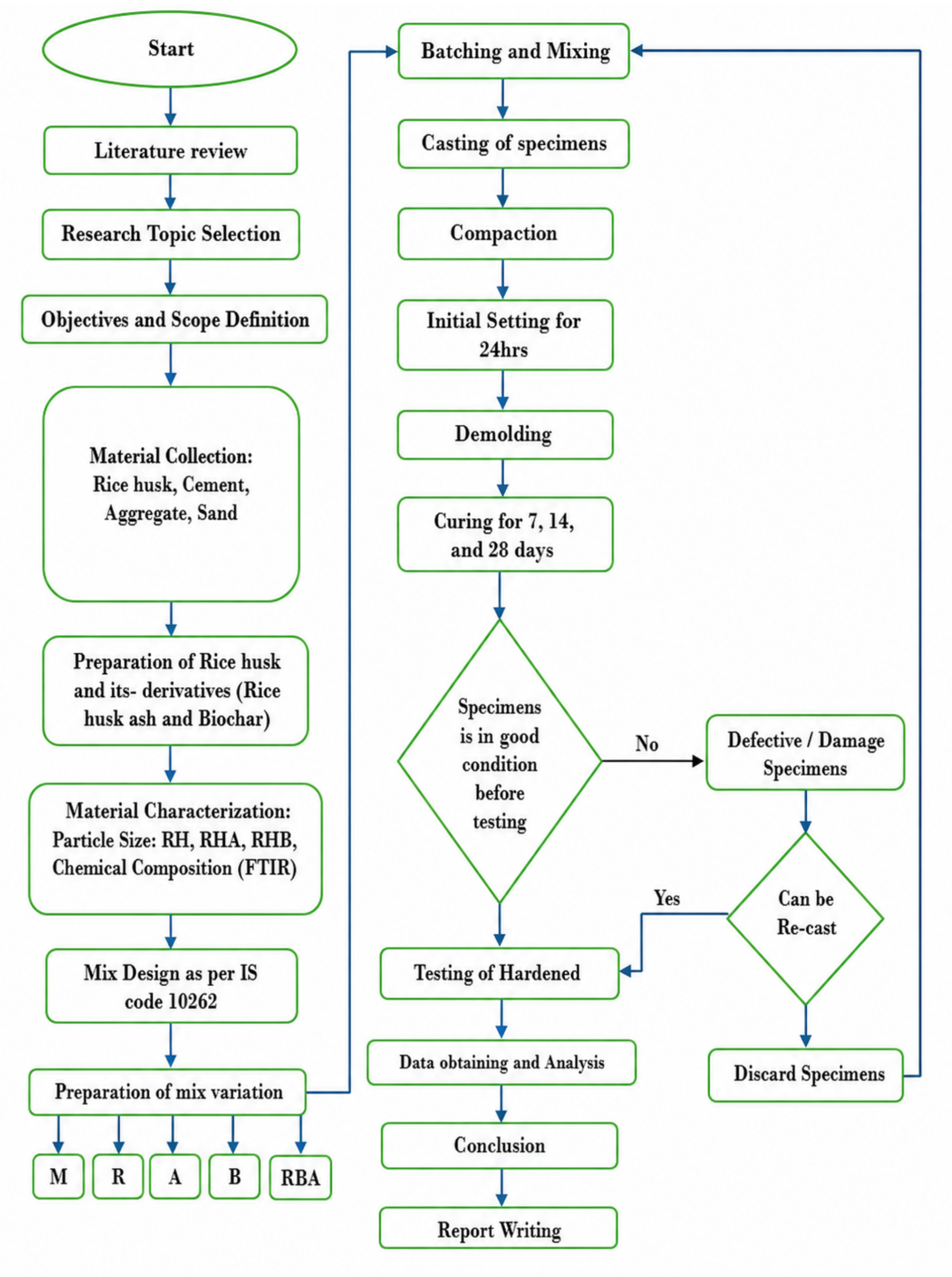

FIGURE 1. Study methodology flowchart

and coarse aggregate, is sourced from Malekhu, Dadhing, and water from reliable sources (Tap Water), ensuring standard specifications.

Preparation of rice husk: Traditionally, the preparation of rice husk and its derivatives at the casting site. This process involves locally processing collected rice husk into usable forms. The collection and cleaning of rice husk from local rice mills at Suryabinayak, Bhaktapur, Nepal. Impurities such as dust, soil, stones, and organic matter are removed manually or by sieving. The rice husk is washed with clean water to eliminate finer contaminants. The cleaned husk is allowed to dry for 24–48 hours at normal atmospheric conditions to remove moisture and ensure proper processing during subsequent stages.
Preparation of rice husk ash: The traditional burning method starts by setting up an open field or a metal drum/kiln at the casting site to produce ash. A perforated base or brick base is provided to allow air circulation with necessary safety measures, including maintaining distance from nearby structures and arranging fire control. The dried rice husk is then ignited, and controlled combustion is maintained by avoiding excessive flames during burning. The temperature range is about 600–700°C. The complete combustion is achieved through slow burning for about 4–6 hours. After burning, the ash is cooled naturally without quenching with water to preserve its pozzolanic properties. The cooled ash is ground manually. A mortar and pestle or grinder is used to grind into finer particle sizes, followed by sieving through a 75-micron sieve to obtain fine rice husk ash comparable to cement particles. The processed ash is stored in an airtight container to prevent moisture absorption and water entrapment.
Preparation of rice husk biochar: The preparation of rice husk biochar through traditional pyrolysis involves the use of a closed metal drum 100 cm in height with small holes of 1 cm in diameter, with a duct pipe of 120 cm height and small holes in the duct of 5 mm diameter throughout the drum center to the base to create a limited oxygen environment. The drum with a 2 cm bottom hole is filled with dried rice husk, ignited through the bottom hole, and then it is partially sealed. The process is carried out under restricted oxygen conditions to avoid complete combustion, maintaining an approximate temperature of 400–500°C. Heating is continued for about 3–5 hours to ensure proper pyrolysis. After completion, the drum is sealed completely with covering mortar and allowed to cool slowly within the chamber, preventing conversion into ash. The obtained biochar is removed and crushed into fine particles. The finer char is sieved to the required size, generally less than 75 microns or as per the required particle size.
Finally, the proper storage of rice husk and its derivatives is necessary to maintain their quality. All the materials are stored separately in dry, airtight containers and labelled appropriately for identification during use. Proper precautions are taken to protect them from moisture and contamination before their use in the concrete preparation.

3.1. **MATERIALS CHARACTERIZATION.** The characterization of incorporated materials used in the mix ensures that it meets the required quality standards. It helps to identify the physical and chemical properties that influence the concrete strength, durability, and workability. The materials considered for characterization include rice husk, rice husk ash, biochar, aggregate (fine and coarse), and water.

3.1.1. *Sieve analysis for incorporated materials.* **Objective:** To determine the fineness or gradation of rice husk, rice husk ash, rice husk biochar, and aggregate (fine and coarse).
Procedure: The standard procedure is used to determine the distribution of particle size of fine aggregate samples. Initially, a series of sieves with aperture sizes of 4.75 mm, 2.36 mm, 1.18 mm, 600 μm, 300 μm, 150 μm, and 75 μm were arranged in descending order, with a collection pan positioned at the bottom. The oven-dried sample 1 was carefully placed on the top sieve and subjected to mechanical vibration for about 10–15 minutes to ensure proper separation of particles according to particle size. The material retained on each sieve was collected separately and weighed with precision after mechanical vibration. Then, the same procedure was carried out for sample 2 under identical testing conditions to maintain consistency and reliability of the results.
The percentages of material retained and passing on each sieve were calculated. Based on these calculations, particle size gradation curves are obtained by plotting the percentage passing against sieve size on a semi-logarithmic graph. The fineness modulus (FM) of each sample was evaluated

using the cumulative percentage retained values. This analysis enabled a grading of the characteristics and suitability of the materials for concrete production.

3.1.2. *Los Angeles' (L.A.) Abrasion Test.* The L.A. Abrasion Test is used to determine the hardness, toughness, and resistance to wear of coarse aggregates.

As per IS 2386 (Part IV), the coarse aggregate sample of about 5000 g was prepared. The aggregate was first sieved to obtain the specified size fraction, generally within the permissible range of 20–25 mm, ensuring uniformity of the test specimen. Then, the prepared sample was placed inside the testing machine along with the twelve hardened steel spheres, which acted as abrasive and impact-producing charges during the test. The drum of the machine was rotated at a speed of about 30–33 rpm for a total of 500 revolutions. Upon completion of the required revolutions, the material was removed from the drum and sieved through a 1.7 mm sieve. The finer particles that passed through the sieve, representing the sample lost due to abrasion and impact, were accurately weighed. The weight loss was subsequently used to determine the L.A. value (percentage), which served as an indicator of the aggregate durability and suitability for use in concrete production.

$$\text{L.A. Abrasion Value (\%)} = \qquad (1)$$

Table 1. Typical Ranges for Aggregate Crushing Value

Aggregate Type	**L.A (in %)**
Very Hard rock	15–20
Medium Hard rock	20–30
Soft rock	30–40

Source: IS code 2386 Part IV

3.1.3. *Aggregate Crushing Value (A.C.V.) test.* The aggregate crushing value (ACV) test was conducted to determine the resistance of coarse aggregate to crushing under a gradually applied compressive load.

For this test, to obtain a uniformly graded sample, aggregate particles passing through a 12.5 mm sieve and retained on a 10 mm sieve were selected. Its initial weight was recorded as W1; the prepared aggregate sample was accurately weighed. The standard cylindrical mold with the aggregate was filled in about 3 equal layers, with each layer compacted by applying 25 uniform blows using a tamping rod to achieve proper packing density. After filling and compaction, the plunger was carefully inserted into the cylinder, and the assembly was positioned in a compression testing machine. A compressive load was applied gradually until a total load of about 40 tons was reached within 10 minutes, as specified in the standard testing procedure. Then, the crushed aggregate was removed from the cylinder and sieved through a 2.36 mm sieve. The finer material that passed through the sieve was collected and weighed as W2.

Aggregate crushing value is calculated by:

$$ACV = \qquad (2)$$

Note: ACV values less than 20% are acceptable.

3.1.4. *Chemical Composition Analysis.* The Chemical Characterization is used to identify chemical constituents that influence cementitious behavior.

The chemical characterization of rice husk and its derivative materials using Fourier Transform Infrared Spectroscopy (FTIR) is carried out to identify the functional groups and chemical bonds present within the samples. The obtained spectra were examined to identify characteristic absorption bands corresponding to various functional groups, including hydroxyl (-OH), siloxane (Si-O-Si), silanol (Si-OH), carbonyl (C=O), and other organic or inorganic constituents. These functional groups provide valuable information regarding the chemical composition and structural changes resulting from the thermal treatment of rice husk. The FTIR spectra obtained for each material (rice husk derivatives) were subsequently compared with established reference spectra and published standards to evaluate their chemical characteristics and pozzolanic potential. Particular attention was given to the presence and intensity of silica-related peaks, as amorphous silica is a key component responsible for pozzolanic activity in cementitious systems.

3.1.5. *Pycnometer Test (Fine Sand).* This method is used to obtain the density related to the water demand of mixed ingredients. Initially, the empty pycnometer was thoroughly cleaned, dried, and weighed as W1. A known quantity of oven-dried sand sample was then placed into the pycnometer, and the combined weight of the pycnometer and the dry sample was measured as W2. Subsequently, the weight of the sand sample was obtained from the difference between W2 and W1. The distilled water was carefully added to the pycnometer containing the sand sample until the calibration mark was reached. Gentle tapping and stirring were carried out to eliminate any entrapped air bubbles, ensuring accurate volume measurement. The exterior surface of the pycnometer was wiped dry, and the weight of the pycnometer containing the sand sample and water was noted as W3. Afterward, the pycnometer was emptied, cleaned, and refilled with distilled water up to the calibration marks. The weight of the pycnometer filled only with water was then measured and recorded as W4. Using the recorded weights, the specific gravity of the sand sample was calculated using the water displaced by the aggregate particles. This test provides an important index property of fine aggregate, which is widely used in concrete mix design, quality control, and the determination of other engineering characteristics of the construction materials. True density of the sample (ρ) is given by:

$$\frac{w_{\text{sample}}}{\left(w_2 - w_1 + w_4 - w_2\right)/\rho_{\text{water}}} \tag{3}$$

Where:
ρ_w = density of water at test temperature (g/cm^3, ~0.998 g/cm^3 at 25°C)

$$W_{\text{sample}} = W_2 - W_1$$

$W_4 - W_3$ accounts for the volume of water displaced by the powder.
Specific Gravity (G) is calculated by:

$$G = \frac{w_2 - w_1}{(w_2 - w_1) - (w_4 - w_3)} \tag{4}$$

3.1.6. *Moisture content test.* Moisture content is determined to identify the amount of water present in aggregate (fine and coarse), which affects the mix water calculations. Samples are dried at 105°C in the oven for 24 hours, and the weight loss is recorded as W2. Sample weight is taken before drying as W1.

$$\text{Moisture content} = \frac{w_1 - w_2}{w_1} \times 100\% \tag{5}$$

3.2. **EXPERIMENTAL ACTIVITIES FOR MIX.** This study was conducted to evaluate the effect of rice husk and its derivatives on the mechanical performance of M20-grade concrete under controlled laboratory conditions in accordance with relevant standard testing procedures. The materials used in the study included ordinary Portland cement (OPC) 43-grade, aggregate (fine and coarse), rice husk, and its derivatives (ash and biochar). The rice husk derivatives, such as rice husk ash, were obtained by controlled combustion of rice husk, while biochar was prepared by pyrolysis under limited oxygen conditions.

A nominal mix M20-grade concrete was adopted for the investigation. A water-cement ratio of 0.50 was maintained throughout the study; however, slight changes in the effective water-cement ratio may have occurred due to the partial replacement of cement with rice husk-based materials. Cement was partially replaced by rice husk derivatives at predetermined replacement levels by weight to evaluate their effects on the fresh and hardened properties of concrete. The freshly prepared concrete mixes were assessed using the slump test in accordance with standard procedures to obtain the workability condition of fresh concrete on site. Concrete cube specimens of 150 mm were cast, compacted, and cured under standard curing conditions for 8, 14, and 28 days. Finally,

the compressive strength of hardened specimens was tested at curing periods of 7, 14, and 28 days using a compression testing machine (CTM). In addition to the mechanical investigations, the chemical and microstructural characteristics of rice husk and its derivatives were analyzed using FTIR to identify the functional groups and assess their potential pozzolanic activity.
The experimental results obtained from workability, compressive strength, and FTIR analyses were systematically evaluated using mean deviation, standard deviation, and error in results and compared with those of the control concrete mix. This comparative assessment facilitated a comprehensive understanding of the effects of rice husk and its derivatives on the performance of M20-grade concrete and their suitability as sustainable supplementary cementitious materials in concrete production.

Table 2. Replacement Material % in Concrete

Mix ID	**Replacement Material**	**Replacement %**
S	Control Mix	0%
R	RH	5%
A	RHA	5%
B	RHB	5%
RBA	RH+RHA+RHB	5%+5%+5%

Table 3. Quantity (kg/m^3) for M20 Concrete

Ingredients of concrete	**Quantity (kg/m^3)**
Cement	383
Fine Aggregate	672
Coarse Aggregate	1196
Water	191
W/C Ratio	0.50

Table 4. Quantity of Material in Modified Mix

Mix ID	**Cement** (kg/m^3)	**RH** (kg/m^3)	**RHA** (kg/m^3)	**RHB** (kg/m^3)	**Water** (kg/m^3)
M	383	0	0	0	191
R	363.85	19.15	0	0	191
A	363.85	0	19.15	0	191
B	363.85	0	0	19.15	191
RBA	325.55	19.15	19.15	19.15	191

Table 5. Number of sample specimens for casting and testing

Mix ID	**7-Days**	**14-Day**	**28-Day**	**Total**
M	3	3	3	9
R	3	3	3	9
A	3	3	3	9
B	3	3	3	9
RBA	3	3	3	9
Total	15	15	15	45

3.3. MIX PROPORTIONING. Quantity of material Calculation for Nominal mix

Target Mean Strength:

$$f'_{ck} = f_{ck} + 1.65S = 20 + 1.65(4) \tag{6}$$

$$= 26.6 \text{ MPa}$$

Water–cement ratio: 0.50
Water = 191 kg/m^3
Cement = $\frac{191}{0.5}$ = 382 kg/m^3
Fine aggregate = 2649 kg/m^3
Coarse aggregate = 1196 kg/m^3
Modified Mix calculation for material quantity
5% replacement:
Cement = 382 − 19.1 = 362.9 kg/m^3
Combined 5% RH + 5% RHA + 5% RHB
Cement = 382 − 57.3 = 324.7 kg/m^3
Quantity calculation for Nominal Mix (M20 150 mm cube specimens)
Cube volume:

$$0.15^3 = 0.003375 \text{ m}^3$$

Total cubes = 45 → Total volume = 0.1519 m^3
Add 10% extra → 0.167 m^3

TABLE 6. Material Calculation for 150 mm cube specimen – 45 cubes

Ingredients of concrete	Quantity (kg)
Cement	63.8 kg
Fine Aggregate	112.2 kg
Coarse Aggregate	199.7 kg
Water	31.9 kg

3.4. **BATCHING, MIXING, CASTING, DE-MOLDING, AND CURING.** The materials such as cement, aggregates, water, and additives were weighed accurately according to the mix design to ensure consistency across all batches. Precise batching is essential to maintain uniformity and accuracy of test results. The materials were thoroughly mixed in a mechanical mixer to achieve a homogeneous concrete or mortar mix. Adequate mixing is critical for both workability and strength, ensuring uniform distribution of cement paste around aggregates. The freshly prepared mix was placed into standard molds (Cube) and compacted properly using a tamping rod or vibrating table to remove air voids, ensuring accurate density and preventing weak zones in the specimen. After the initial setting period (typically 24 hours), the specimens were carefully removed from the molds to avoid damage. De-molding allows the samples to retain their shape for subsequent curing and testing. The removed mold specimens were immersed in water or kept in a moist environment for the required curing periods (7, 14, 28 days), allowing the cement to hydrate. Proper curing ensures maximum strength development and durability of the concrete.

3.5. **TESTING OF CUBES.**

3.5.1. *Codes.*

TABLE 7. Laboratory testing Standards and IS codes

Test / Procedure	**IS Code**
Plain & Reinforced Concrete – Code of Practice	IS 456:2000
Concrete Mix Design	IS 10262:2019
Sampling and Analysis of Concrete	IS 1199:2018
Compressive Strength Test	IS 516:2018
OPC 43 Grade Cement Specification	IS 8112:2013
Aggregate Specification	IS 383:2016
Cement Testing Methods	IS 4031

3.5.2. *Fresh concrete testing (Slump test).* According to IS 1199:2018, the test was conducted to evaluate the workability of fresh concrete under laboratory conditions. The test was performed using standard apparatus, including a slump cone with a tamping rod, base plate, and measuring scale. The slump cone was placed on a level base plate and filled with fresh concrete in three equal layers, compacted by tamping with 25 blows of a standard tamping rod for each layer. After filling and levelling the top layer or surface, the cone was carefully lifted vertically, allowing the concrete to spill. The vertical height difference between the height of the cone and the displaced concrete was measured with a scale, which represents the slump value, indicating the workability of the concrete mix.

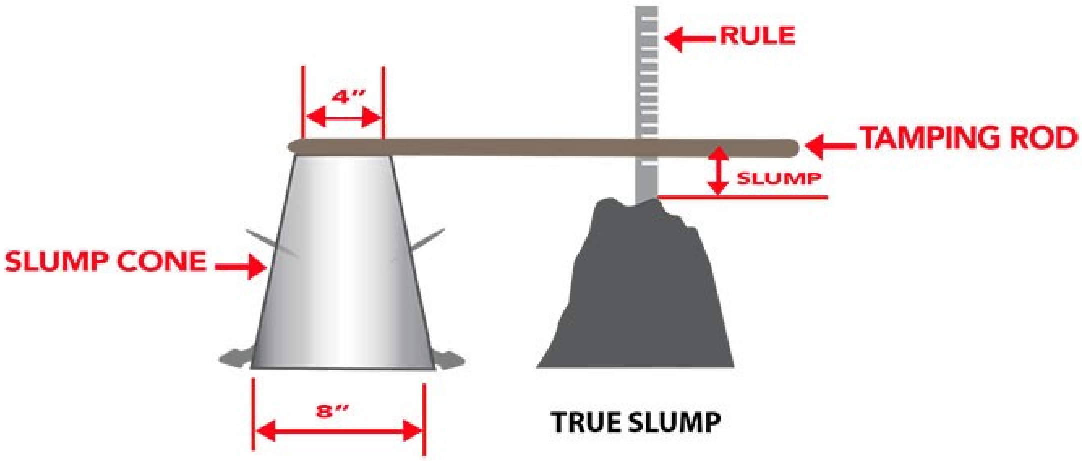

FIGURE 2. Slump cone setup to measure slump (source: google.docs.com/image)

3.5.3. *Hardened concrete testing (compressive strength test).* Compressive strength tests were carried out on 150 mm concrete in accordance with IS code 516:2028. The specimens were cured for 7, 14, and 28 days before testing. During testing, the load was applied gradually using a compression testing machine (UTM) until failure occurred, and the maximum load was recorded. The compressive strength of the concrete was then determined using the following relation:

$$F_c = \frac{P}{A} \tag{7}$$

Where:
f_c = Compressive strength (MPa)
P = Maximum applied load (N)
A = Cross-sectional area of cube (mm^2)
For a 150 mm cube:

$$A = 150 \times 150 = 22500 \text{ mm}^2$$

4. DATA ANALYSIS, RESULTS, AND DISCUSSION

The results and discussion of M20 concrete incorporating RH, RHA, and RHB as partial cement replacements. Material and Mix Performance evaluation includes:

(1) Cement, Aggregate, Sand, RH, RHA, RHB testing
(2) Workability (slump test)
(3) Compressive strength at 7, 14, and 28 days
(4) Microstructural characterization (FTIR)

The effects of individual and combined replacements were compared with the control mix.

4.1. **Cement testing result.** The physical and mechanical properties of the cement used in the experimental work were obtained from the manufacturer's test certificate issued by Hongshi Shivam Cement Pvt. Ltd. The certificate provided essential quality-control parameters, including normal consistency, setting time (initial and final), soundness, and compressive strength at different curing periods, for ensuring compliance with the relevant provisions of NS 572:2076 for 43-grade Ordinary Portland Cement (OPC).
The test results are presented in Table 8, demonstrating that the cement meets the required criteria specified by NS 572:2076. The normal consistency of 26.9% indicates a typical water demand for achieving a standard paste consistency. The initial setting time (IST) and final setting time (FST) were recorded as 220 and 280 minutes, respectively, providing sufficient time for mixing, placing, and finishing concrete. The soundness value of cement is 0.5 mm, reflecting volumetric stability and suggesting a low risk of undesirable expansion after hardening. The compressive strength values obtained at curing periods of 3, 7, and 28 days were 30.7 MPa, 39.0 MPa, and 54.7 MPa, respectively, indicating a consistent and satisfactory rate of strength development throughout the curing age. In particular, the 28-day compressive strength significantly exceeds the minimum specified requirement of 43.58MPa for 43-grade cement, confirming the high quality and strength-producing capability of the material.

Table 8. Physical Requirements of Cement

Property	**Requirement as per NS 572:2076 (43 grade)**	**Testing Result**
Normal Consistency (%)	-	26.9
Initial Setting Time (Min)	≥ 45	220
Final Setting Time (Min)	≤ 600	280
Soundness (Le Chatelier) (mm)	≤ 10	0.5
Compressive Strength – 3 days (MPa)	≥ 23.0	30.7
Compressive Strength – 7 days (MPa)	≥ 33.0	39.0
Compressive Strength – 28 days (MPa)	43.58	54.7

Finally, the cement was considered suitable for M20-grade concrete production for study and for evaluating the effects of rice husk and its derivatives as partial replacement materials.

4.2. Aggregate Testing Results.

4.2.1. *Los Angeles' Abrasion Value (L.A).* The L.A. Abrasion value is calculated by:

$$\text{L.A. Abrasion Value (\%)} =$$

TABLE 9. Observation and Calculation Table for L.A. ACV

Sample ID	Aggregate Size (mm)	Weight Before Test (g)	Weight of Fines Passing 1.7 mm Sieve (g)	L.A. (%)	Remarks
AG-01	20–25	5000	750	15.0	Good resistance
AG-02	20–25	5000	900	18.0	Medium resistance
AG-03	20–25	5000	1200	24.0	Slightly soft
AG-04	20–25	5000	1500	30.0	Soft rock

The test result presented in Table 9, evaluates the resistance of coarse aggregate to wear, abrasion, and impact. The result ranged from 15% to 30% for the aggregate samples. Among them, AG-01 showed the lowest abrasion value of 15%, indicating excellent resistance to wear and impact, while AG-04 recorded the highest abrasion value of 30%, suggesting comparatively lower durability. Samples AG-02 and AG-03 produce intermediate abrasion values of 18% and 24%, respectively, demonstrating moderate resistance to abrasion.

Overall, the increase in abrasion value indicates a reduction in aggregate hardness and durability. The results suggest that AG-01 and AG-02 have better mechanical properties and are more suitable for the required higher durability and wear resistance. The results highlight the importance of aggregate quality in influencing the long-term performance of concrete.

4.2.2. *Aggregate crushing test by the Crushing Machine.* **Sample 1**
Original Sample weight (W1) = 300g
Weight of fine sand after passing through 2.36 sieve (W2) = 22g

$$ACV = \frac{W_2}{W_1} \times 100 = \frac{22}{300} \times 100 = 7.33\%$$

Sample 2
Original Sample weight (W1) = 300g
Weight of fine sand after passing through 2.36 sieve (W2) = 23.5 g

$$ACV = \frac{W_2}{W_1} \times 100 = \frac{23.5}{300} \times 100 = 7.83\%$$

Average ACV = 7.58%

The aggregate crushing value (ACV) test was performed to determine the resistance of coarse aggregate to crushing under a gradually applied compressive load. The results obtained are presented in the above calculation. Sample 1 recorded as ACV of 7.33%, whereas sample 2 recorded a slightly higher value of 7.83%. The average ACV of the tested aggregate was 7.58%. According to IS 2386 (Part IV): 1963, aggregates with a lower crushing value possess greater strength and more resistance to crushing under load. Generally, aggregates with an ACV of less than 10% are considered exceptionally strong, while values up to 30% are suitable for concrete used in wearing surfaces and structural applications. In this study, the average ACV is subsequently below these allowable limits, indicating excellent aggregate quality.

For both samples, the low crushing values indicate that the aggregate has high mechanical strength and toughness, and it is capable of withstanding heavy compressive loads without significant disintegration. Such an aggregate contributes to improved concrete strength, durability, and long-term performance. Based on the test results and the requirements of IS 2386 (Part IV), the aggregate used can be classified as very strong and highly suitable for high-quality concrete production.

4.2.3. *Specific Gravity of Sand Using the Pycnometer Method.* Weight of Empty Pycnometer (W1) is 650g, Weight of Pycnometer+dry sand (W2) is 1150g, Weight of Pycnometer+sand+water (W3) is 1458g, Weight of pycnometer filled with water (W4) is 1338g.
Then,

$$\text{Weight of dry sand (Ws)} = W_2 - W_1 = 1150 - 650 = 500g$$

$$\text{Weight of water (Ww)} = (W_4 - W_1) - (W_3 - W_2) = 380g$$

$$\text{Specific gravity of sand (G)} = \frac{W_s}{W_w} = \frac{500}{380} = 2.63$$

The specific gravity of the fine aggregate obtained was 2.63, which lies within the permissible range specified for commonly used construction sand.

Table 10. Specific gravity of different types of sand

Types of sand	**Specific gravity**
Natural River sand	2.55–2.70
Crushed sand	2.50–2.75
Clean Quartz sand	2.60–2.65

Referring to Table 10, the Specific gravity values provide a standard reference for evaluating the quality and suitability of fine aggregate used in concrete. The obtained value lies within the permissible range of 2.55–2.70 for natural river sand and 2.60–2.65 for clean quartz sand, indicating that the sand possesses normal density and contains a sound mineral composition suitable for concrete production.

Table 11. Sieve analysis for sample 1

Sample 1 (S1)				
Sieve Size (mm)	**Wt. (g)**	**% Ret.**	**Cum. % Ret.**	**% Pass**
4.75	0	0.0	0.0	100.0
2.36	20	2.0	2.0	98.0
1.18	90	9.0	11.0	89.0
0.600	220	22.0	33.0	67.0
0.300	300	30.0	63.0	37.0
0.150	250	25.0	88.0	12.0
0.075	90	9.0	97.0	3.0
Pan	30	3.0	100.0	0.0
Total	1000	100		

4.3. **Fine aggregate testing.** In Table 11, the sieve analysis results for fine aggregate sample 1, the majority of fine particles are distributed between 0.600mm and 0.300mm sieves, indicating proper gradation and gradual variation in particle sizes. The cumulative percentage is retained uniformly, and the percentage passing decreases steadily, indicating a well-graded material. Only 3% passes through the 0.075 mm sieve, showing low fines content. Overall, the sample exhibits suitable grading characteristics for use as fine aggregate in a concrete mix.
The sieve analysis results for fine aggregate sample 2 (Table 12) show that the percentage passing at all sieve sizes falls within the IS grading Zone II limits. The values closely follow the specific ranges from 4.75mm to 0.15mm, indicating a well-graded aggregate. All sieve sizes comply with IS 838 requirements, confirming uniform particle distribution and suitable grading. Therefore, sample 2 is appropriate for use as fine aggregate in concrete.

Table 12. Sieve analysis data and calculation for sample 2

Sample 2 (S2)				
Sieve Size (mm)	**Wt. (g)**	**% Ret.**	**Cum. % Ret.**	**% Pass**
4.75	0	0.0	0.0	100.0
2.36	25	2.5	2.5	97.5
1.18	85	8.5	11.0	89.0
0.600	210	21.0	32.0	68.0
0.300	310	31.0	63.0	37.0
0.150	245	24.5	87.5	12.5
0.075	95	9.5	97.0	3.0
Pan	30	3.0	100.0	0.0
Total	1000	100		

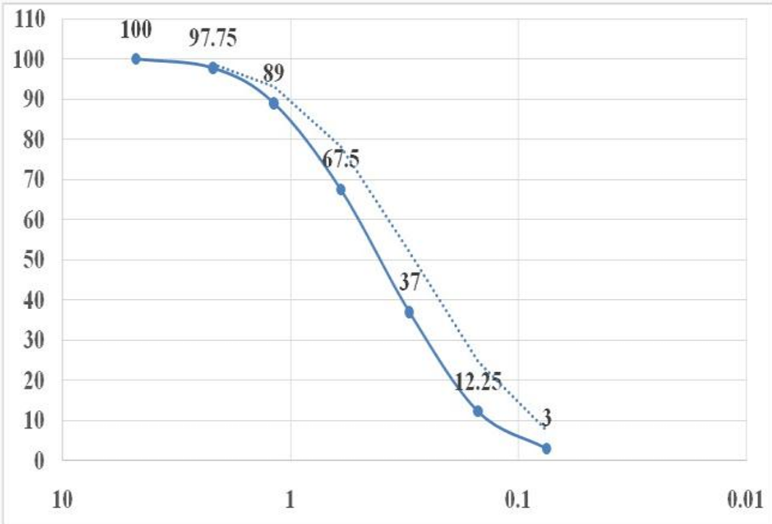

Figure 3. Particle size distribution curves for fine sand samples (S1 and S2) showing similar gradation and uniformity of source material.

Table 13. Grain size distribution parameters of fine sand

Parameter	Value
Coefficient of Uniformity (C_u)	15.29
Coefficient of Curvature (C_c)	2.95
Fineness Modulus	1.96

Figure 3 shows the particle size distribution curves for fine sand samples (S1 and S2), indicating similar gradation and uniformity of the source material.
The gradation parameters shown in Figure 3 and Table 13 indicate a coefficient of uniformity (C_u) of 15.29 and a coefficient of curvature (C_c) of 2.95, indicating a well-graded fine aggregate. The fineness modulus of 1.96 suggests relatively fine sand. Based on the sieve analysis results, the aggregate meets Zone II requirements and is suitable for use as fine aggregate in a cementitious system.

4.4. **Fresh Concrete Testing (Workability Test–Slump Test).** The slump test results from Table 14 indicate that the control mix (M) exhibits the highest workability with a slump of 25 mm. Incorporation of rice husk slightly reduces the slump to 23 mm, while rice husk ash shows a

TABLE 14. Observation table of slump for mixes

Mix ID	Mix Description	Slump (mm)
M	Control Concrete	25
R	5% RH	23
A	5% RHA	14
B	5% RHB	17
RBA	RH+RHA+RHB	16

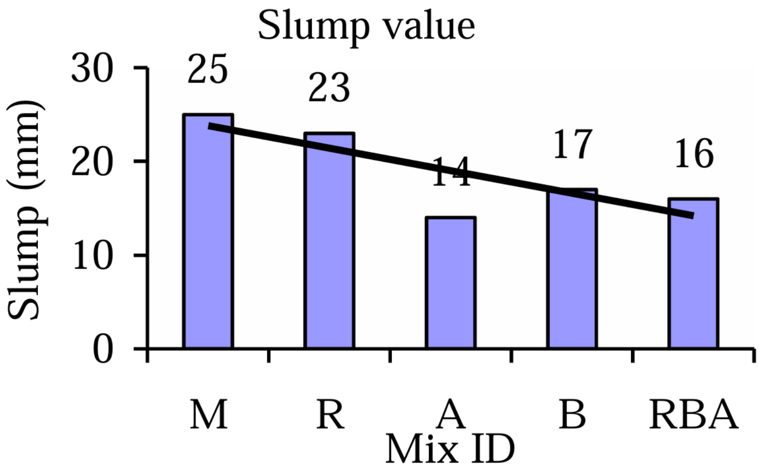

FIGURE 4. Variation of slump value for different concrete mixes

significant reduction to 14 mm due to its finer particles and higher water demand. Rice husk biochar also reduces workability to 17 mm because of its porous nature. The combined mix (RBA) records a slump of 16 mm and shows moderate workability. Overall, the inclusion of rice husk and its derivatives decreases workability compared to conventional concrete.
Figure 4 shows the variation of slump value for different concrete mixes.
The slump value decreases from mix R (23 mm) to mix A (14 mm), then slightly increases for mix B (17 mm) and remains moderate for the combined mix RBA (16 mm), indicating reduced workability with the addition of rice husk derivatives.
The average slump of the concrete mixes was 19.0 mm, indicating relatively low workability compared to the control mix. The standard deviation of 4.74 mm shows moderate variation among the slump values of different mix compositions, while the coefficient of variation of 24.97% suggests variability in workability due to the incorporation of rice husk and its derivatives. The standard error of 2.12 mm indicates that the estimated mean slump value is reasonably reliable. The reduction in slump from the control mix (M) to the modified mixes can be attributed to the higher water absorption capacity and larger specific surface area of rice husk-based materials, which reduce the free water available for lubrication within the concrete matrix. Therefore, the results demonstrate that the addition of rice husk and its derivatives affects fresh concrete workability and may require water adjustment or admixture use to maintain the desired consistency.

4.5. **Hardened Cube Specimen Testing.** The compressive strength of concrete is defined as the ability of concrete to withstand axial compressive loads, which is used to assess its quality and performance. Concrete cube specimens of standard size (150 mm cube) were tested under a compression testing machine after specified curing periods (7, 14, and 28 days). The load was applied gradually until failure occurred, and the maximum load at failure was recorded for each specimen as P kN. The cube failure pattern was also observed, typically showing diagonal cracks

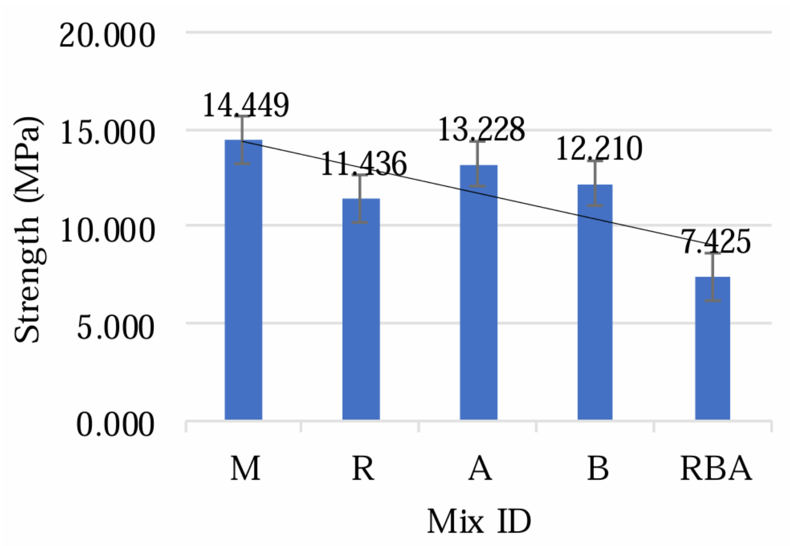

FIGURE 5. 7 - day compressive strength of conventional and modified mix

or crushing, indicating proper load application and uniform distribution. The final compressive strength is reported as the average of three specimens for each mix proportion and curing period (7, 14, and 28 days).

TABLE 15. 7-day Strength observation and calculation

Mix ID	Failure Load (P) kN	Strength (f) N/mm^2	Average Strength N/mm^2	Deviation in Strength	% Change in Strength
M1	326.5	14.511	14.449	0	0.00%
M2	325.2	14.453			
M3	323.6	14.382			
R1	258.2	11.476	11.436	-3.013	-20.86%
R2	257.6	11.449			
R3	256.1	11.382			
A1	299.1	13.293	13.228	-1.221	-8.44%
A2	297.4	13.218			
A3	296.4	13.173			
B1	274.3	12.191	12.210	-2.239	-15.50%
B2	277.5	12.333			
B3	272.4	12.107			
RBA1	169.5	7.533	7.425	-7.024	-49.61%
RBA2	163.4	7.262			
RBA3	168.3	7.480			

From Table 15, the compressive strength results show that the control mix (M) achieved the highest average strength of 14.449 N/mm^2, indicating good early strength development. However, the mix (R) exhibited a significantly lower strength of 11.436 N/mm^2, representing a reduction of approximately 20–21% compared to the control mix. Similarly, Mix A achieved a strength of 13.228 N/mm^2, which performed better than Mix R but remained slightly lower than the control mix M, indicating moderate strength improvement.

Similarly, Mix B recorded a strength of 12.210 N/mm^2, showing intermediate performance, higher than Mix R but lower than both Mix A and Mix M. Therefore, the combined mix RBA exhibited the lowest strength of 7.425 N/mm^2, showing a significant reduction of approximately 48–50% compared to the control mix. This reduction may be attributed to weaker bonding and increased porosity within the concrete matrix.

Figure 5 shows that the error bars for all mixes are relatively small, indicating low variation in strength and good consistency in the test results. The control mix M and Mix A exhibit slightly smaller error bars, suggesting more uniform strength among samples. Mix R and B show

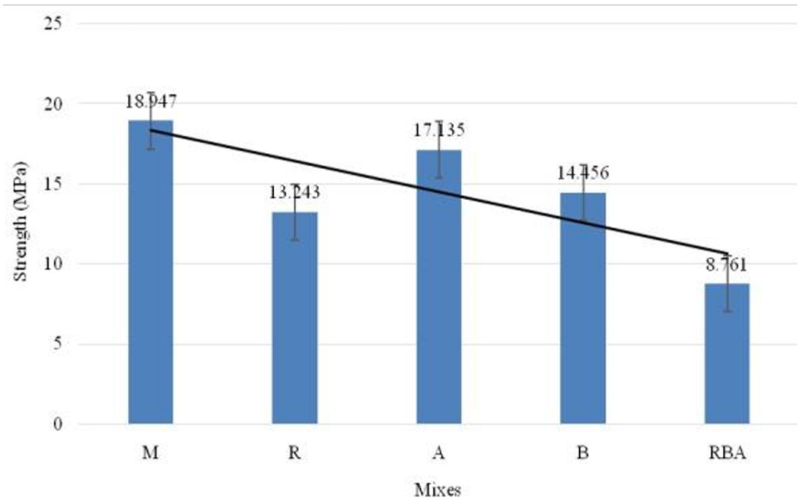

FIGURE 6. 14-day compressive strength of different concrete mixes

moderate variation, while the RBA mix has slightly larger error bars, indicating comparatively higher variability in the results. Overall, the narrow error bars reflect reliable and consistent experimental measurements.

Table 15 and Figure 5 show the 7-day strength behavior at early curing age for all modified mixes, demonstrating a reduction in strength compared to the control mix M. The highest reduction is observed in the RBA mix (-48.61%), indicating slower early hydration and weaker initial binding. Mix R also shows a notable reduction (-20.86%), whereas Mix A performs comparatively better with only an 8.44% reduction.

TABLE 16. 14-day Strength observation and calculation

Mix ID	Failure Load (P) kN	Strength (f) N/mm^2	Average Strength N/mm^2	Deviation in Strength	% Change in Strength
M4	426.6	18.960	18.947	0	0.00%
M5	426.9	18.973			
M6	425.4	18.907			
R4	296.7	13.187	13.243	-10.148	-53.54%
R5	299.3	13.302			
R6	297.9	13.240			
A4	384.3	17.080	17.135	-1.812	-9.56%
A5	387.1	17.204			
A6	385.2	17.120			
B4	323.5	14.378	14.456	-4.491	-23.70%
B5	327.1	14.538			
B6	325.2	14.453			
RBA4	197.9	8.796	8.761	-10.186	-53.75%
RBA5	196.1	8.716			
RBA6	197.4	8.773			

Table 16 shows the 14-day compressive strength results, where the control mix M achieved the highest strength (18.947 N/mm^2), followed by Mix A (17.135 N/mm^2). Mix B (14.456 N/mm^2) and Mix R (13.243 N/mm^2) showed moderate strength, while the combined mix RBA exhibited the lowest strength (8.761 N/mm^2), indicating a significant reduction.

Figure 6 shows the trend line of the 14-day compressive strength graph, which indicates a gradual decreasing pattern from mix M to RBA. This demonstrates a reduction in strength with increasing modification or replacement level. Mix M exhibits the highest strength and forms the starting point of the downward trend, while RBA shows the lowest strength and weakest performance at this curing age.

In terms of error bars, mixes such as R and RBA show relatively larger variations, indicating higher inconsistency in the results, whereas Mix M and Mix A display smaller error bars, reflecting

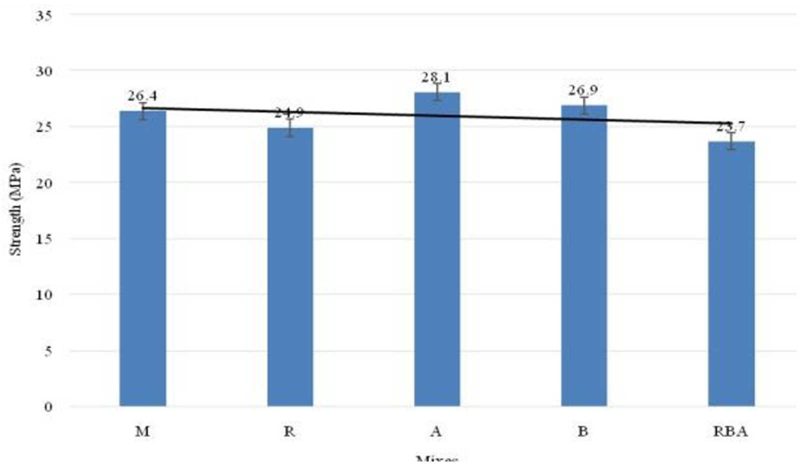

FIGURE 7. 28-day compressive strength of Conventional and modified mix.

more stable and reliable behavior. Overall, the graphs suggest that compressive strength decreases progressively with mix modification, while variability tends to increase in modified mixes.
Table 16 and Figure 6 elaborate on the 14-day strength behavior and 14-day strength development; the trend continues, and remains lower than the control for most mixes. R and RBA mixes show severe reduction (>53%), indicating delayed strength gain. Mix A, indicating relatively stable behavior, 9.56% reduction in strength, suggests better pozzolanic reaction, compared to other mixes.

TABLE 17. 28-day Strength observation and calculation

Mix ID	Failure Load (P) (kN)	Strength (f) (N/mm^2)	Average strength (N/mm^2)	Deviation in strength	% Change in strength
M7	594.0	26.400	26.407	0.0	0.00%
M8	596.5	26.511			
M9	592.0	26.311			
R7	558.0	24.800	24.874	-1.5	-5.68%
R8	561.0	24.933			
R9	560.0	24.889			
A7	630.0	28.000	28.089	+1.7	+6.44%
A8	634.0	28.178			
A9	632.0	28.089			
B7	605.0	26.889	26.911	+0.5	+1.89%
B8	607.5	27.000			
B9	604.0	26.844			
RBA7	532.0	23.644	23.644	+2.7	-10.23%
RBA8	534.0	23.733			
RBA9	530.0	23.556			

From Table 17, the 28-day compressive strength results show that mix A achieved the highest average strength (28.0889N/mm^2), followed by mix B (26.911N/mm^2) and the control mix M(26.089N/mm^2). The mix R recorded slightly lower strength (24.876N/mm^2), while the mix RBA showed the lowest strength (23.644 N). Overall, Mix A demonstrates the best strength performance at 28 days.
Figure 7 shows the 28-day compressive strength graph with slight changes in strength without a clear continuous decrease in all mixes. The results of Mix A exhibit the highest strength, followed by Mix B and Mix M, while Mix RBA shows the lowest strength, indicating comparatively weaker mechanical performance at this curing period of 28-days. The overall pattern suggests that certain modifications (especially in Mix A) can enhance strength, while others (RBA) may reduce it.
Table 17 and Figure 7 show that 28-day strength behavior and long-term strength development become more visible. Mix A compared to the control with +6.44% gain, indicating effective pozzolanic contribution from the ash contained in rice husk ash. Mix B also slightly exceeds

Table 18. Observation table of slump for mixes

Mix ID	Mix Description	Slump (mm)
M	Control Concrete	25
R	5% RH	23
A	5% RHA	14
B	5% RHB	17
RBA	RH+RHA+RHB	16

control by +1.89% due to pore refinement by rice husk biochar and water entrapped in the biochar. However, RBA shows a slight decrease by 10.23%, and R remains slightly lower by 5.68%, indicating incomplete strength recovery in these replacement mixes.
Strength Trend: RHA > RHB > Control > RH > combined mix

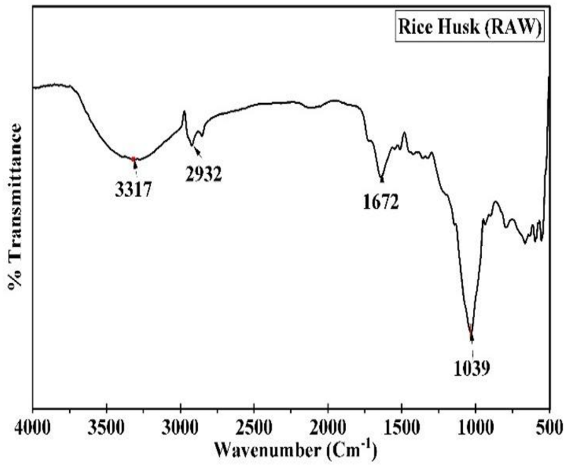

Figure 8. FTIR spectrum of Rice husk (raw)

4.6. **Microstructural Analysis (FTIR characterization) of incorporating materials (Rice husk and its derivatives).** Figure 8 shows the major functional groups present in the material, a broad absorption band with 3317 cm^{-1}, corresponding to the stretching vibration of hydroxyl groups, indicating the presence of cellulose, hemicellulose, absorbed moisture, and lignin. The peak near 2932 cm^{-1} indicates C–H stretching vibrations of aliphatic compounds, confirming the existence of organic compounds in the biomass material, such as rice husk (raw).
Figure 8 also shows that the FTIR spectrum displays a peak at 1672 cm^{-1}, which is related to carbonyl groups associated with lignin and hemicellulose. A peak at 1039 cm^{-1} is associated with Si–O–Si and Si–O stretching vibrations, indicating the high amount of silica present in the rice husk. The results indicate that rice husk contains both organic and silica-rich inorganic elements, highlighting its potential as a precursor material or for additional cementitious applications in the concrete mix for modification of concrete as used for supplementary cementitious materials.

4.7. **Fresh concrete testing (Workability test- Slump test).** The slump test results from Table 18 indicate that the control mix (M) exhibits the highest workability with a slump of 25mm. Incorporation of rice husk slightly reduces the slump to 23mm, while rice husk ash shows a significant reduction to 14mm due to its finer particles and higher water demand. Rice husk biochar also reduces workability to 17mm because of its porous nature. The combined mix (RBA) records a slump of 16mm and shows moderate workability. Overall, the inclusion of rice husk and its derivatives decreases workability as compared to a conventional concrete mix.

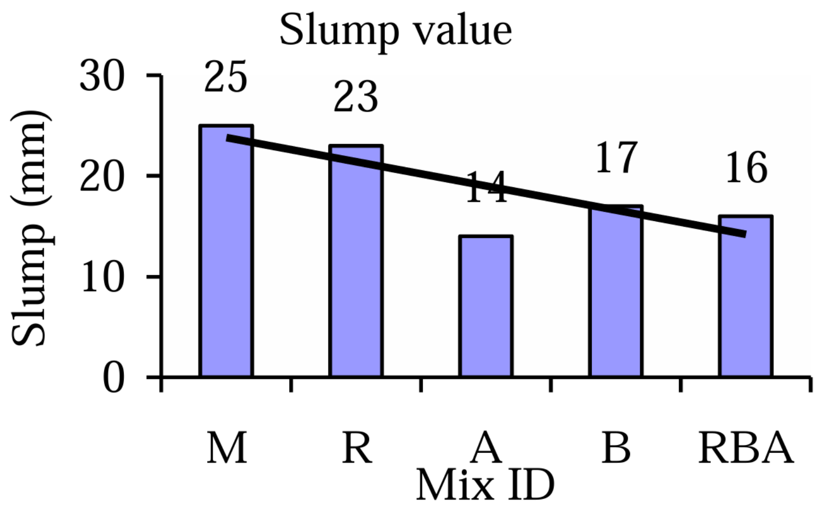

Figure 9. Variation of slump value for different concrete mixes

Figure 9, showing that the slump value decreases from mix R (23mm) to mix A(16mm), then slightly increases for mix B(17mm) and remains moderate for the combined mix RBA (16mm), indicating reduced workability with the addition of rice husk derivatives.

The average slump of the concrete mixes was 19.0mm, indicating relatively low workability as compared to the controlled mix. The standard deviation of 4.74mm shows moderate variation among the slump values of different mix compositions, while the coefficient of variation of 24.97% suggests variability in workability due to the incorporation of rice husk and its derivatives. The standard error of 2.12mm, indicating that the estimated mean slump value is reasonably reliable. The reduction in slump from the control mix (M) to the modified mixes can be attributed to the higher water absorption capacity and larger specific surface area of rice husk-based materials, which tend to reduce the free water available for lubrication within the concrete matrix. Therefore, the results demonstrate that the addition of rice husk - its derivatives affects fresh concrete workability and may require water adjustment or admixture use to maintain the desired consistency.

4.8. **E. Hardened Cube Specimen Testing.** The compressive strength of concrete is defined as the ability of concrete to withstand axial compressive loads, which is used to assess its quality and performance. Concrete cube specimens of standard size (150mm cube) under a compression testing machine after a specified curing period (7, 14, and 28 days) were tested with the load applied gradually until failure occurred. The maximum load at failure was recorded for each specimen as P KN. The cube failure pattern was also observed, typically showing diagonal cracks or crushing, indicating proper load application and uniform distribution. The final compressive strength is reported as the average of three specimens for each mix proportion and curing period (7, 14, and 28 days).

From Table 19, the compressive strength results show that the control mix (M) achieved the highest average strength of 14.449 N/mm^2, indicating good early strength development, but the mix (R) exhibited a significantly lower strength of 11.436 N/mm^2, representing a reduction of about 20–21% compared to the control mix. Similarly, Mix A has a strength of 13.228 N/mm^2, performed better than Mix R but remained slightly lower than the control mix M, indicating moderate strength improvement.

Similarly, Mix B noted a strength of 12.210N/mm^2, showing intermediate performance, higher than Mix R but lower than both Mix A and Mix M. Therefore, the combined mix RBA exhibited the lowest strength of 7.425N/mm^2, showing a significant reduction of approximately 48–50%

Table 19. 7-day Strength observation and calculation

MIX ID	Failure Load (P) KN	Strength (f) N/mm^2	Average Strength N/mm^2	Deviation in strength	% Change in strength
M1	326.5	14.511	14.449	0	0.00%
M2	325.2	14.453			
M3	323.6	14.382			
R1	258.2	11.476	11.436	-3.013	-20.86%
R2	257.6	11.449			
R3	256.1	11.382			
A1	299.1	13.293	13.228	-1.221	-8.44%
A2	297.4	13.218			
A3	296.4	13.173			
B1	274.3	12.191	12.210	-2.239	-15.50%
B2	277.5	12.333			
B3	272.4	12.107			
RBA1	169.5	7.533	7.425	-7.024	-49.61%
RBA2	163.4	7.262			
RBA3	168.3	7.480			

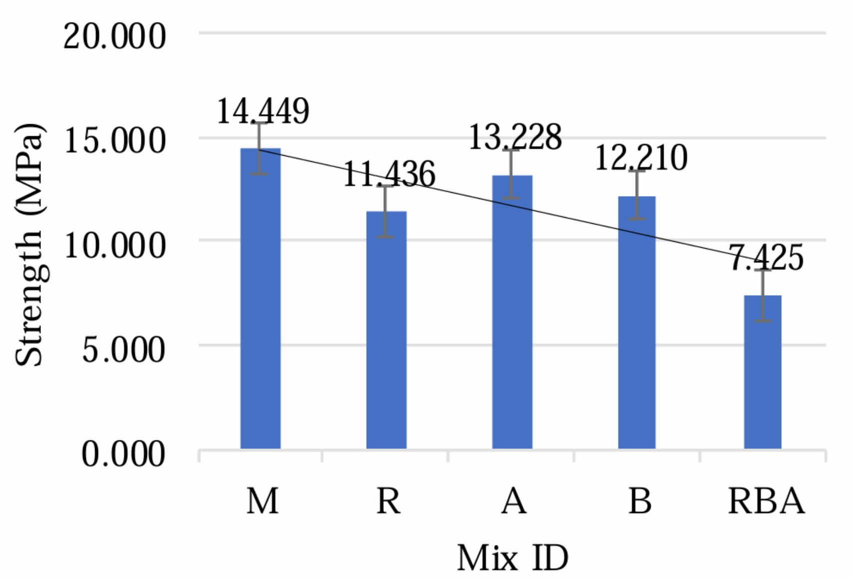

Figure 10. 7-day compressive strength of conventional and modified mix

compared to the control mix, which may be attributed to weaker bonding and increased porosity in the concrete matrix.

Figure 10 shows that the error bars for all mixes are relatively small, indicating low variation in strength and good consistency in the test results. The control mix M and Mix A exhibit slightly smaller error bars, suggesting more uniform strength among samples. Mix R and B shows moderate variation, while the RBA mix has slightly larger error bars, indicating comparatively higher variability in the results. Overall, the narrow error bars reflect reliable and consistent experimental measurements.

Table 19 and Figure 10 show the 7-day strength behavior at early curing age for all modified mixes, showing a reduction in strength compared to M. The highest reduction is observed in RBA mix (-48.61%), indicating slower early hydration and weaker initial binding, while Mix R also shows a notable drop (-20.86%), but Sample A performs comparatively better with only -8.44% reduction.

Table 20 shows the 14-day compressive test, in which the control mix M has the highest strength (18.947 N/mm^2), followed by the mix A(17.135N/mm^2). Mix B (14.456 N/mm^2) and Mix R (13.243 N/mm^2) show moderate strength, while the combined mix RBA has the lowest strength (8.761N/mm^2), indicating a significant reduction.

Figure 11 shows the trend line in the 14-day compressive strength graph, which shows a gradual decreasing pattern from mix M to RBA, indicating a reduction in strength with increasing

Table 20. 14-days Strength observation and calculation

MIX ID	Failure Load (P KN)	Strength (f) N/mm^2	Average strength N/mm^2	Deviation in strength	% Change in strength
M4	426.6	18.960	18.947	0	0.00%
M5	426.9	18.973			
M6	425.4	18.907			
R4	296.7	13.187	13.243	-10.148	-53.54%
R5	299.3	13.302			
R6	297.9	13.240			
A4	384.3	17.080	17.135	-1.812	-9.56%
A5	387.1	17.204			
A6	385.2	17.120			
B4	323.5	14.378	14.456	-4.491	23.70%
B5	327.1	14.538			
B6	325.2	14.453			
RBA4	197.9	8.796	8.761	-10.186	-53.75%
RBA5	196.1	8.716			
RBA6	197.4	8.773			

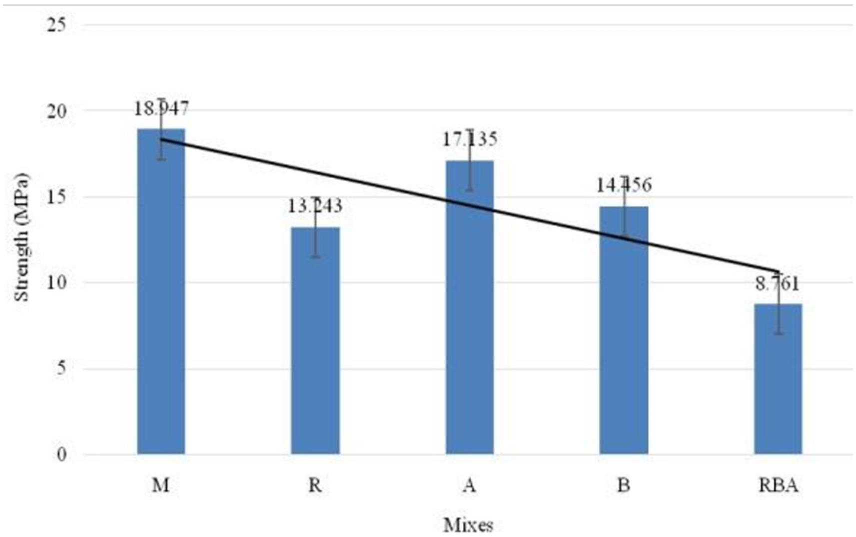

Figure 11. 14-day compressive strength of different concrete mixes

modification or replacement. The mix M exhibits the highest strength, and forms the starting point of the downward trend, while RBA shows the lowest strength, the weakest performance at this curing age. In terms of error bars, mixes such as R and RBA show relatively larger changes, indicating inconsistency in the results at a higher level, but mix M and A display smaller error bars, reflecting more stable and reliable behavior. Overall, the graphs suggest that the strength decreases progressively with mix modification, while variability tends to increase in the altered mixes.

Table 20 and Figure 11 elaborate on the 14-day strength behavior and 14-day strength development; the trend continues, and remains lower than the control for most mixes. R and RBA mixes show severe reduction (¿53%), indicating delayed strength gain. Mix A, indicating relatively stable behavior, 9.56% reduction in strength, suggests better pozzolanic reaction, compared to other mixes.

From Table 21, the 28-day compressive strength results show that mix A achieved the highest average strength (28.0889N/mm^2), followed by mix B (26.911N/mm^2) and the control mix M(26.089N/mm^2). The mix R recorded slightly lower strength (24.876N/mm^2), while the mix RBA showed the lowest strength (23.644 N). Overall, Mix A demonstrates the best strength performance at 28 days.

Figure 12 shows the 28-day compressive strength graph with slight changes in strength without a clear continuous decrease in all mixes. The results of Mix A exhibit the highest strength, followed

TABLE 21. 28-days Strength observation and calculation

MIX ID	Failure Load (P) KN	Strength (f) N/mm^2	Average strength N/mm^2	Deviation in strength	% Change in strength
M7	594.0	26.400	26.407	0	0.00%
M8	596.5	26.511			
M9	592.0	26.311			
R7	558.0	24.800	24.874	-1.5	-5.68%
R8	561.0	24.933			
R9	560.0	24.889			
A7	630.0	28.000	28.089	+1.7	+6.44%
A8	634.0	28.178			
A9	632.0	28.089			
B7	605.0	26.889	26.911	+0.5	+1.89%
B8	607.5	27.000			
B9	604.0	26.844			
RBA7	532.0	23.644	23.644	+2.7	-10.23%
RBA8	534.0	23.733			
RBA9	530.0	23.556			

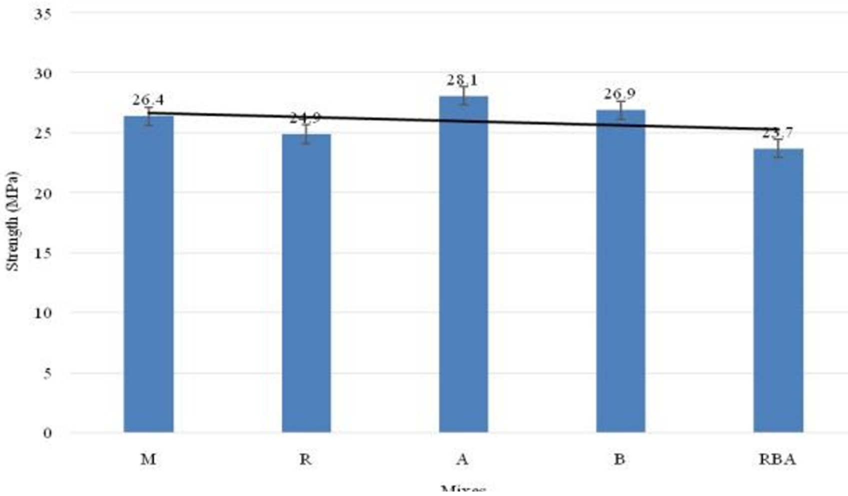

FIGURE 12. 28-day compressive strength of Conventional and modified mix

by Mix B and Mix M, while Mix RBA shows the lowest strength, indicating comparatively weaker mechanical performance at this curing period of 28-days. The overall pattern suggests that certain modifications (especially in Mix A) can enhance strength, while others (RBA) may reduce it.
Table 21 and Figure 12 show that 28-day strength behavior and long-term strength development become more visible. Mix A compared to the control with +6.44% gain, indicating effective pozzolanic contribution from the ash contained in rice husk ash. Mix B also slightly exceeds control by +1.89% due to pore refinement by rice husk biochar and water entrapped in the biochar. However, RBA shows a slight decrease by 10.23%, and R remains slightly lower by 5.68%, indicating incomplete strength recovery in these replacement mixes.
Strength Trend: RHA > RHB > Control > RH > combined mix

4.9. **Microstructural Analysis (FTIR characterization) of incorporating materials (Rice husk and its derivatives).** Figure 13 shows the major functional groups present in the material, a broad absorption band with 3317 cm^{-1}, corresponding to the stretching vibration of hydroxyl groups, indicating the presence of cellulose, hemicellulose, absorbed moisture, and lignin. The peak near 2932 cm^{-1} indicates C-H stretching vibrations of aliphatic compounds, confirming the existence of organic compounds in the biomass material, such as rice husk (raw).
Figure 13 also shows that the FTIR spectrum displays a peak at 1672 cm^{-1}, which is related to carbonyl groups associated with lignin and hemicellulose. A peak at 1039 cm^{-1} is associated with Si-O-Si and Si-O stretching vibrations, indicating the high amount of silica present in the rice husk. The results indicate that rice husk contains both organic and silica-rich inorganic elements,

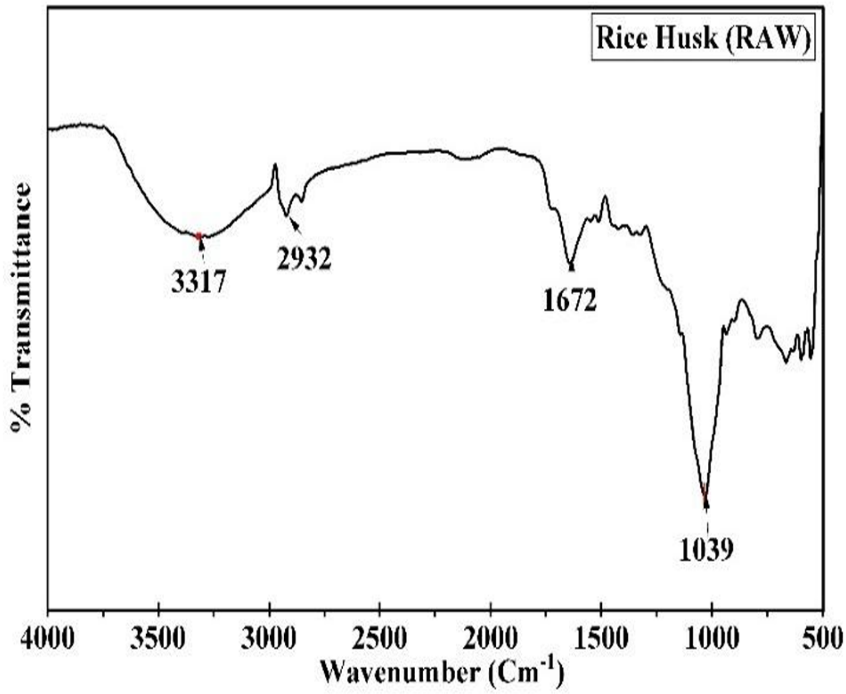

Figure 13. FTIR spectrum of Rice husk (raw)

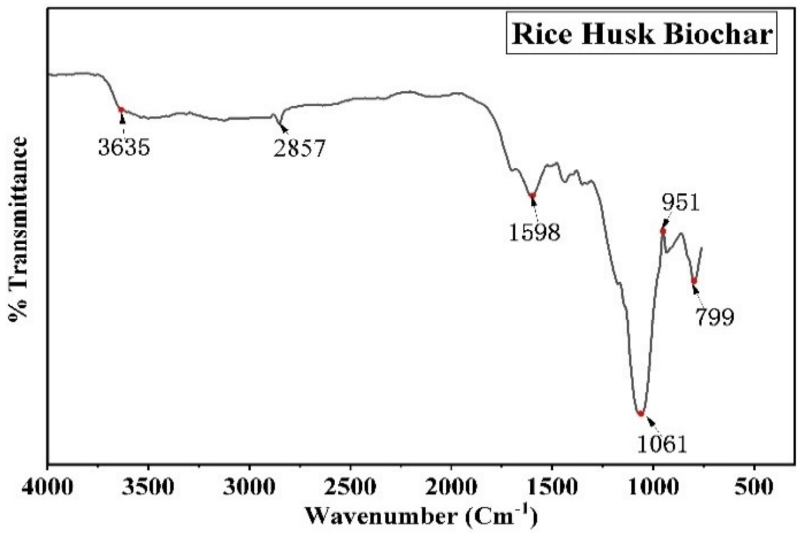

Figure 14. FTIR spectrum of Rice husk biochar

highlighting its potential as a precursor material or for additional cementitious applications in the concrete mix for modification of concrete as used for supplementary cementitious materials.
Figure 14 shows the FTIR spectrum of rice husk biochar with peaks at 3635, 2857, 1598, 1061, 951, and 799 cm^{-1}. The peaks at 3635 cm^{-1} indicate O-H stretching, 2971 cm^{-1}corresponds to C-H stretching, and 1677 cm^{-1} represents C=C or aromatic bonding associated with aromatic carbon structures and carbonyl groups formed after thermal treatment. The strong peak at 1031 cm^{-1} confirms Si-O-Si vibrations, indicating the presence of Silica in the biochar. Compared to raw RH,

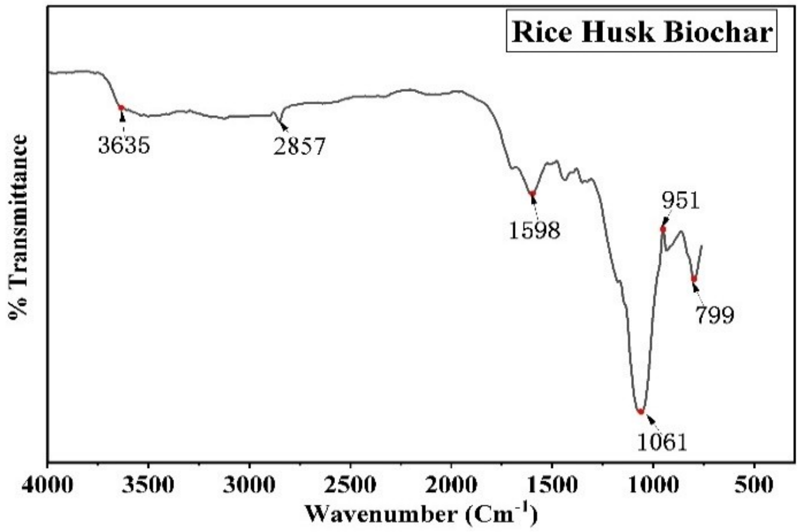

FIGURE 15. FTIR spectrum of Rice husk ash and biochar

TABLE 22. Important FTIR Peaks in RH, RHA, and RHB

Wavenumber (cm^{-1})	Functional Group	Interpretation
3400–3600	O–H stretching	Moisture/hydroxyl groups
1500–1700	H–O–H bending	Water molecules
1000–1200	Si–O–Si stretching	Silica structure
600–900	Si–O vibration	Quartz phase
200–500	Si–O bending	Silicate

the reduced intensity of this peak suggests the decomposition of volatile organic compounds during carbonization.

Figure 15 and Table 22 show that the strong absorption peak at 1031cm^{-1} is assigned to Si-O-Si stretching vibrations, confirming the presence of silica. This peak is more intense in rice husk ash, indicating a higher silica content and enhanced pozzolanic potential. Similarly, biochar exhibits relatively lower intensity in this region, reflecting its higher carbon content and lower silica dominance, which is also crucial for concrete modification. Overall, the results confirm rice husk ash is rich in silica, while rice husk biochar retains more carbon-based functional groups and acts as a pozzolanic material (ash).

According to Table 22, the FTIR analysis identifies the key functional groups and silica-related compounds found in RH, RHA, and RHB samples. The large peak at 3400–3600 cm^{-1} shows O-H stretching, indicating moisture and hydroxyl groups. H-O-H bending vibrations interconnected to water molecules are shown by the peak at 1500–1700 cm^{-1}. The presence of silica structure is confirmed by a strong peak between 1000–1200 cm^{-1}, indicating Si-O-Si stretching. The lower range of 200–500 cm^{-1} corresponds to Si-O bending vibrations, representing silicate compounds in the materials, whereas the peaks between 600–900 cm^{-1} represent Si-O vibrations associated with quartz phases.

5. CONCLUSION AND RECOMMENDATION

5.1. **A. Conclusion.** This study investigated the influence of rice husk (RH) and its derived forms, rice husk ash (RHA) and rice husk biochar (RHB), on the fresh, mechanical, and microstructural

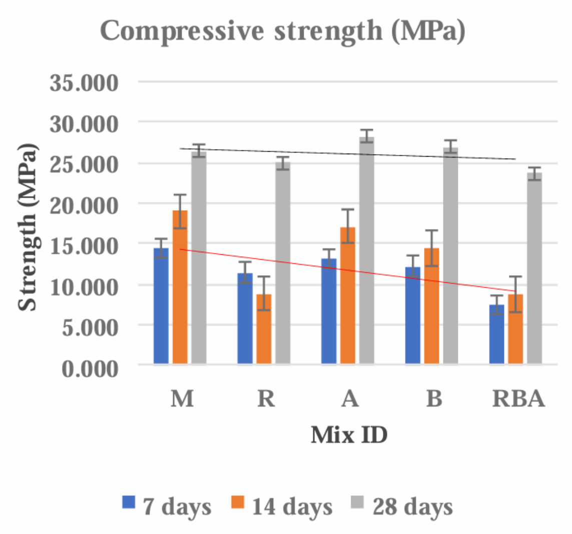

FIGURE 16. Strength of M20 conventional and modified concrete

properties of M20 grade concrete. Clearly stated that the experimental results showed that the incorporation of rice husk-based materials generally reduced workability. The slump values decreased progressively from the control mix to the modified mixes, with the lowest workability observed in the combined mix. Mainly, this reduction is associated with the higher surface area, porous nature, and increased water absorption capacity of the agricultural waste-based additives, which demand more mixing water and reduce concrete flowability.

In terms of compressive strength, the results revealed that a limited replacement level of RHA significantly enhanced concrete performance. The mix A achieved the highest 28-day compressive strength of 28.1 MPa, representing an improvement over the control mix, indicating the effectiveness of pozzolanic reaction and micro-filler action in densifying the cement matrix. A marginal improvement in strength was observed in the combined RHB mix, attributed to enhanced silica availability due to controlled thermal processing. In contrast, the reduction in compressive strength is due to the presence of untreated organic matter in RH, lower reactivity. The combined RH + RHA + RHB mix exhibited the lowest compressive strength, attributed to excessive cement replacement, increased porosity, and reduced hydration products due to binder dilution.

Further, FTIR analysis confirmed the presence of reactive silica phases in RHA and RHB samples, with prominent Si–O–Si bonding vibrations indicating strong pozzolanic potential present in the husk and acting as pozzolanic materials such as SCM's. These microstructural observations support the improved strength performance of the optimized mixes, while weaker structural characteristics in the combined mix explain its lower mechanical performance. Additionally, promoting agricultural waste in construction reduces environmental impact.

Finally, the study concludes that 5% RHA replacement is the most suitable proportion for enhancing the mechanical performance of M20 concrete in terms of strength and microstructure while maintaining acceptable workability. Although RHB can be used as a supplementary material, excessive or combined replacement beyond optimal levels is not recommended due to its negative impact on hydration and concrete density. The findings of this research support the careful optimization of agricultural waste-based materials to achieve durable, eco-friendly, and high-performance concrete systems. The major findings of the study indicate that the workability of the concrete decreases slightly with the incorporation of rice husk and its derivatives. The combined mix shows the lowest slump, while mix B remains closer to the control mix, indicating relatively better workability among the modified mixes.

TABLE 23. Workability and Strength Summary

Mix	**Workability**	**Strength Performance**
M	Good	Reference
R	Slightly reduced	Moderate
A	Lower slump	Highest
B	Good slump	Comparable
RBA	Lowest slump	Slightly lower

Based on the results presented in the data analysis, results, and discussion chapter, it is also observed that the presence of silica in RHA plays a significant role in enhancing the pozzolanic activity, contributing to the overall performance of the concrete.
Table 23 presents the overall performance of different concrete mixes in terms of workability and strength. The control mix M shows good workability as well as serving as the reference for strength comparison with modified mix specimens. The results of Mix R exhibit a slight reduction in workability and moderate strength behavior, while Mix A has a lower slump, indicating reduced workability, but achieves the highest strength among all mixes. Furthermore, Mix B maintains a good slump with strength comparable to the control mix (M).

5.2. **Recommendation.** The recommendations have been made based on the study performed:

(1) The 5% rice husk ash is partially replaced by weight of cement, which is optimal for M20 concrete.
(2) Rice husk and biochar are safe at 5% replacement for minor environmental conditions.
(3) Combined replacement $> 10\%$ should be carefully controlled, but if made, then admixture must be used.
(4) Further research is needed for the assessment of durability tests, hybrid mixes, advanced microstructural analysis (SEM, TEM, TGA), and life cycle assessment with the economic analysis for the mass production and field application.

Ash and Biochar enhanced the strength and sustainability for the partial replacement of cement in M20 concrete mix, while maintaining acceptable workability, but the raw husk is not suitable for the cementitious material, as it acts as a filler in the concrete.

References

[1] P. K. Mehta and P. J. M. Monteiro, *Concrete: Microstructure, Properties and Materials*, 4th ed. New York, NY, USA: McGraw-Hill Education, 2014.
[2] A. M. Neville, *Properties of Concrete*, 5th ed. Harlow, U.K.: Pearson Education, 2011.
[3] A. A. Ramezanianpour, *Cement Replacement Materials.* Berlin, Germany: Springer, 2014.
[4] M. Thomas, *Supplementary Cementing Materials in Concrete.* Boca Raton, FL, USA: CRC Press, 2013.
[5] M. Amran, S. Debbarma, and T. Ozbakkaloglu, "Rice husk ash-based concrete composites: A critical review of their properties and applications," *Materials*, vol. 14, no. 3, pp. 1–35, 2021.
[6] S. Barbhuiya *et al.*, "Rice husk ash in structural concrete: Influence on strength, durability and sustainability," *Discover Concrete and Cement*, vol. 1, no. 14, pp. 1–18, 2025.
[7] S. Chandrasekhar, P. N. Pramada, and L. Praveen, "Processing, properties and applications of reactive silica from rice husk–an overview," *Journal of Materials Science*, vol. 38, pp. 3159–3168, 2012.
[8] K. Ganesan, K. Rajagopal, and K. Thangavel, "Rice husk ash blended cement: Assessment of optimal level of replacement for strength and permeability properties of concrete," *Construction and Building Materials*, vol. 22, no. 8, pp. 1675–1683, 2008.
[9] G. A. Habeeb and H. B. Mahmud, "Study on properties of rice husk ash and its use as cement replacement material," *Materials Research*, vol. 13, no. 2, pp. 185–190, 2010.
[10] A. Mugahed *et al.*, "Rice husk ash-based cement composites: A review of mechanical and durability performance," *Crystals*, vol. 11, no. 2, p. 168, 2021.
[11] A. Kumar and B. Singh, "Influence of rice husk ash on strength and durability of concrete," *Journal of Materials in Civil Engineering*, vol. 30, no. 4, p. 04018029, 2018.
[12] M. Safiuddin and N. Hearn, "Comparison of rice husk ash and silica fume in cement composites," *Cement and Concrete Research*, vol. 40, pp. 418–426, 2010.

[13] V. Sata, C. Jaturapitakkul, and K. Kiattikomol, "Utilization of rice husk ash in high-strength concrete," *Construction and Building Materials*, vol. 31, pp. 332–338, 2012.

[14] N. Van Tuan, G. Ye, K. Van Breugel, and A. Fraaij, "The study of rice husk ash as supplementary cementitious material in concrete," *Cement and Concrete Research*, vol. 41, no. 3, pp. 301–307, 2011.

[15] P. Vignesh and K. Vivek, "Study on strength properties of concrete using rice husk ash," *International Journal of Engineering Research and Technology*, vol. 4, no. 3, pp. 238–242, 2015.

[16] M. H. Zhang and V. M. Malhotra, "High-performance concrete incorporating rice husk ash as supplementary cementing material," *ACI Materials Journal*, vol. 93, no. 6, pp. 629–636, 2010.

[17] S. Gupta and H. W. Kua, "Factors determining the potential of biochar as a carbon-capturing construction material," *Journal of Materials in Civil Engineering*, vol. 29, no. 9, pp. 1–12, 2017.

[18] X. Tan, Y. Liu, Y. Gu *et al.*, "Biochar-based materials in sustainable construction applications: A review," *Construction and Building Materials*, vol. 325, p. 126748, 2021.

[19] K. L. Scrivener, R. Snellings, and B. Lothenbach, *A Practical Guide to Microstructural Analysis of Cementitious Materials*. Boca Raton, FL, USA: CRC Press, 2016.

[20] ASTM International, "Astm c39/c39m-23: Standard test method for compressive strength of cylindrical concrete specimens," ASTM International, West Conshohocken, PA, USA, Tech. Rep., 2023.

[21] Bureau of Indian Standards, "Is 456:2000 – plain and reinforced concrete – code of practice," Bureau of Indian Standards, New Delhi, India, Tech. Rep., 2000.

[22] ——, "Is 10262:2019 – concrete mix proportioning guidelines," Bureau of Indian Standards, New Delhi, India, Tech. Rep., 2019.

[23] ——, "Is 383:2016 – specification for coarse and fine aggregates from natural sources for concrete," Bureau of Indian Standards, New Delhi, India, Tech. Rep., 2016.

[24] ——, "Is 516:1959 – methods of tests for strength of concrete," Bureau of Indian Standards, New Delhi, India, Tech. Rep., 1959.

[25] ——, "Is 1199:1959 – methods of sampling and analysis of concrete," Bureau of Indian Standards, New Delhi, India, Tech. Rep., 1959.

[26] ASTM International, "Astm c618: Standard specification for coal fly ash and raw or calcined natural pozzolan for use in concrete," ASTM International, West Conshohocken, PA, USA, Tech. Rep.

[27] S. Sharma and R. Khan, "Use of agricultural waste in concrete: A review," in *Proceedings of International Conference on Sustainable Construction Materials*, 2017, pp. 45–52.